Anal. Chem. **2010,** *82,* 8476–8484

Relationship between MALDI IMS Intensity and Measured Quantity of Selected Phospholipids in Rat Brain Sections

Joseph A. Hankin and Robert C. Murphy*

Department of Pharmacology; University of Colorado Denver; Mail Stop 8303, Aurora, Colorado 80045

MALDI IMS positive ion images of rat brain show a regional distribution of phosphocholine species that is striking in the apparent distinctiveness and reproducibility of such depictions. The interpretation of these images, specifically the relationship between MALDI IMS ion intensity and the amount of the phosphocholine (PC) species in the tissue is complicated by numerous factors, such as ion suppression, ion molecule chemistry, and effects of tissue structure. This study was designed to test the hypothesis that the intensity of PC molecular species does relate to the quantity of molecules in a tissue sample. A set of comparison studies for a limited but representative selection of cell-derived PC molecular species was carried out using LC/MS/MS to measure the amounts of these species in brain tissue extracts. There was good correlation between the MALDI IMS ion abundance of PC molecular species and the relative abundance of corresponding PC molecular species in microdissected regions analyzed by LC/MS/MS.

MALDI imaging mass spectrometry (MALDI IMS) involves compilations of MALDI mass spectra acquired sequentially in a two-dimensional array and reprocessed to display signal intensities for specific ions at each coordinate position.[1,2] Rodent brain tissue sections (rat or mouse) have been frequently used for mass spectral imaging studies because of availability, ease of histological preparations, abundance and diversity of lipids, and for morphological regional contrasts that lend themselves to intriguing images.[3−7] In all of these MALDI IMS studies of rodent brain the glycerophosphocholine (PC) molecular species have been observed as the most abundant positive ions desorbed from all regions of the brain sample.[3] These abundant signals for PC show regional intensity contrasts that are striking in their visual correspondence to stained sections of the same tissue. Such depictions of regional distinctiveness appear to be independent of matrix applications, instrumentation, and even different ionization methods such as MALDI, SIMS,[8] or DESI.[9] There have been consistent results of an apparent discrete detection of specific PC molecules in different regions of brain tissue including detailed fine structures.[4] The overall visual impression of processed MALDI mass-specific images suggests that there are different abundances of specific PC molecules in different regions of brain. However, the validity of these visual impressions in brain tissue has yet to be verified by independent measurements of the regional sections. Caprioli et al.[10] recently reported good correspondence between MALDI MS image intensities and measured amounts of specific phospholipids molecules in developing mouse embryos.

There are numerous complicating factors that could affect the comprehensiveness of MALDI MS images.[11] Brain tissue has differentiated regional substructures with heterogeneous cell types. Differences in cell density or intercellular spacing could affect matrix deposition and desorption of the cell lipids. Furthermore, the complex mixture of lipids in brain when analyzed by mass spectrometry is subjected to competing ionization and ion−molecule chemistry that can result in nonlinear relationships between the ion signal from each compound and the true quantity of a molecule present in the sample. Another complication has been that phospholipids appear in MALDI IMS studies as sodium or potassium adducts of PC along with the protonated form. The source of potassium or sodium has been presumably from the buffering salts of inter- and intra- cellular fluids. Because a gradient of Na^+ and K^+ concentrations is actively maintained across living cell membranes, the tissue preparation and the depth of sampling in the MALDI event all could cause variability in the availability of alkali metal salts on the sample. These different layers of complexity when analyzing a sample of rodent brain tissue make it difficult to interpret MALDI IMS data in terms of lipid concentration. Yet, the visual clarity, and reproducibility

* To whom correspondence should be addressed. Tel: 303-724-3352. Fax: 303-724-3357. E-mail: Robert.Murphy@ucdenver.edu.

(1) Cornett, D. S.; Reyzer, M. L.; Chaurand, P.; Caprioli, R M. *Nat. Methods* **2007**, *4*, 828–833.
(2) Amstalden van Hove, E. R.; Smith, D. F.; Heeren, R. M. *J. Chromatogr. A.* **2010**, *1217*, 3946–3954.
(3) Hankin, J. A.; Barkley, R. M.; Murphy, R. C. *J. Am. Soc. Mass Spectrom.* **2007**, *18*, 1646–1652.
(4) Sugiura, Y.; Konishi, Y.; Zaima, N.; Kajihara, S.; Nakanishi, H.; Taguchi, R.; Setou, M. *J. Lipid Res.* **2009**, *50*, 1776–1788.
(5) Jackson, S. N.; Wang, H. J.; Woods, A. S. *J. Am. Soc. Mass Spectrom.* **2005**, *16*, 2052–2056.
(6) Garrett, T. J.; Prieto-Conaway, M. C.; Kovtoun, V.; Bui, H.; Izgarian, N.; Stafford, G.; Yost, R. A. *Int. J. Mass Spectrom.* **2007**, *260*, 166–176.
(7) Puolitaival, S. M.; Burnum, K. E.; Cornett, D. S.; Caprioli, R. M. *J. Am. Soc. Mass Spectrom.* **2008**, *19*, 882–886.
(8) Heien, M. L.; Piehowski, P. D.; Winograd, N.; Ewing, A. G. *Methods Mol. Biol.* **2010**, *656*, 85–97.
(9) Wiseman, J. M.; Ifa, D. R.; Cooks, R. G. *J. Am. Soc. Mass Spectrom.* **2010**, *21*, 1177–1189.
(10) Burnum, K. E.; Cornett, D. S.; Puolitaival, S. M.; Milne, S. B.; Myers, D. S.; Tranguch, S.; Brown, H. A.; Dey, S. K.; Caprioli, R. M. *J. Lipid Res.* **2009**, *50*, 2290–2298.
(11) Heeren, R. M.; Smith, D. F.; Stauber, J.; Kükrer-Kaletas, B.; MacAleese, L. *J. Am. Soc. Mass Spectrom.* **2009**, *20*, 1006–1014.

10.1021/ac101079v
Published on Web 09/20/2010

of images of brain tissue suggest a stability of systematic events that when better understood would assist interpretation of the images.

This study was designed to test the hypothesis that intensity of PC molecular species in MALDI IMS does relate to the absolute quantity of molecules in a tissue sample. A set of comparison studies for a limited but representative selection of cell-derived phosphatidylcholine molecular species was carried out. The relative quantities of these phospholipids extracted from microdissected regions of rat brain and analyzed by LC/MS were compared systematically to a series of corresponding MALDI MS images and the abundance of corresponding MALDI ions.

EXPERIMENTAL SECTION

Materials. Methanol (CH_3OH) and methylene chloride (CH_2Cl_2) used for lipid extractions and HPLC were purchased from Fisher Scientific (Fairlawn, NJ) as HPLC grade of purity and used without further purification. Water was purified by a Millipore (Billerica, MA) filtration system to 18 mΩ resistance. Ammonium acetate was purchased from Fisher Scientific and Hanks Balanced Salt Solution (HBSS) from MediaTech (Herndon, NJ). The MALDI matrix 2,5-dihydroxybenzoic acid (DHB) was purchased from ACROS Organics (Morris Plains, NJ). The LC/MS/MS internal standard ($[^2H_6]$-16:0/16:0 PC) was purchased from Avanti Polar Lipids (Alabaster, AL). MALDI plates used for tissue imaging were smooth surfaced stainless steel Opti-TOF inserts (Applied Biosystems, Thornhill, Ontario, Canada).

Tissue Preparation and Sectioning. Two female Sprague−Dawley rats were euthanized (isofluorine, followed by decapitation) and the intact brains were dissected immediately, bisected into hemispheres, laid into small, plastic trays, and frozen in crushed dry ice and stored at −70 C° until sectioning. Sectioning was carried out by mounting the brain hemisphere onto a cryostat chuck with OCT, without embedding the tissue. Frozen sections were collected beginning 1 mm lateral to midline with the following sequence: two 10 μm slices for application to a MALDI plate, two 10 μm slices for application to glass slides for H&E staining,[12] one thick section (0.5 mm) for microdissection, two 10 μm slices on glass slides for H&E staining, and two final 10 μm slices on a MALDI plate for imaging. This sequence was repeated in different animals three additional times thus giving four complete sets of samples. Images and stained sections acquired before and after the 0.5 mm slice were compared to ensure correspondence between larger microdissected sections used for LC/MS/MS and LC/MS analysis and the corresponding MALDI images.

Tissue Extraction. The regions chosen for analysis by microdissection were determined based on contrasting intensities in previously acquired mass spectrometric images, as well as ease of dissection under a dissecting microscope. Thick (0.5 mm) tissue slices were manually cut from the sectioning block with a razor blade, placed onto a glass slide, flash frozen and stored at −70 C° until needed. Microdissection was carried out using previously described methods.[13] Briefly, the tissue on the glass slide was placed onto a styrofoam tray with a frozen 'cold pack' on the bottom and pieces of dry ice around the periphery. The vaporizing CO_2 helped to maintain a minimal amount of water condensation during the dissection, and the cold pack maintained a cold temperature at approximately −5 C°, warm enough to cut the tissue, yet cold enough to maintain tissue integrity. The sections were microdissected with the assistance of a mechanical dissection tool (Transferman, Eppendorf, Hamburg Germany) using the tip of a 26 gauge syringe needle as the cutting knife. Tissue sections were transferred cold into a preweighed, precleaned glass vial, weighed, flash frozen in liquid nitrogen, and pulverized with a Teflon tipped syringe plunger. The crushed tissue in the vial was suspended in 200 μL CH_3OH, 100 μL HBSS, and 100 μL CH_2Cl_2 (modified Bligh/Dyer extraction) with additional methanol dripped in as needed to form a monophase solution. Internal standard ($[^2H_6]$-DPPC) was added (25 ng), and the solution was vortexed for 30 s. Further tissue homogenization was carried out with multiple 20 s bursts with a probe sonicator at 15% power intensity. Addition of 100 μL of deionized H_2O and 100 μL of CH_2Cl_2 induced phase separation, and 60 μL of the lower layer were removed and placed into a Teflon capped autosampler vial for normal phase chromatography.

Mass Spectrometry: MALDI IMS. MALDI TOF analysis used for tissue imaging was carried out on a QStar XL QqTOF instrument using Analyst QS software with O-MALDI server 5.1 (Applied Biosystems). A solid state high repetition laser operated at 500 Hz, 8.2 μJ, with a 0.5 s acquisition time and a nitrogen laser (20 Hz, 40 μJ, 0.5 s acquisition) were used in this study. Conditions for acquisition in positive ion mode included a focusing potential (FP) of 60, declustering potential (DP2) 20, curtain gas of 25 units. Collisional activation experiments were carried out using argon as collision gas with a voltage drop of 30−50 across the collision cell (Q2). For positive ion images, DHB matrix was applied using sublimation under reduced pressure (50 mTorr) at 120 C° for 11 min.[3] Images were acquired at 75 μm plate movement steps, and typically took 10−12 h to acquire across the 20 × 12 mm^2 area of the sample surface. The MALDI data were processed from raw data to "analyze" format using a "wiff to analyze" script provided by Applied Biosystems/MDS Sciex at a resolution of 10 data points/amu and viewed using Tissue View software (Applied Biosystems). The images presented have not been smoothed, normalized or preprocessed.

Normalization and Processing of MALDI IMS Data. The signal intensities of four MALDI MS images used in this study were significantly different due to different lasers and different laser power output through the course of this study. A normalization factor was applied to these images to bring them within scale of each other for statistical analysis. To do this, a region of interest (ROI) was manually drawn around the entire processed image and mass spectral signal was averaged for the region. The processed signal at any mass had a finite width of 0.3 amu, so a range of digitized intensity numbers associated with a single m/z value (i.e.760.6 ± 0.1) were summed. These summed signals for each ionized form of 16:0/18:1 PC ($[M + H]^+$ m/z 760.6, $[M + Na]^+$ m/z 782.6, $[M + K]^+$ m/z 798.6) were combined and this number was used to normalize the intensity of each image. The 16:0/18:1 PC is a common and prominent component of

(12) Kiernan, J. A. *Histological and Histochemical Methods: Theory and Practice*, 4th ed.; Scion: Bloxham, U.K., 2008.
(13) Axelsen, P. H.; Murphy, R. C. *J. Lipid Res.* **2010**, *51*, 660–671.

cell membranes, and generated an abundant signal in all images that was predominantly free of other contributing isobaric species. Normalization of spectra to a common and abundant phospholipid component instead of total signal or an external standard[14] was rationalized as a fair method for this study given proposed comparisons within this class of molecule, presumed possible effects from chemical interferences, and the potential for signal differences because of tissue structures. The use of summed signal of all forms ($[M + H]^+$, $[M + Na]^+$, $[M + K]^+$) of 16:0/18:1 PC for the normalization factor arose subsequent to observations of significant sample to sample variability in the alkali ion forms and that the summation of all forms reduced variability in data analysis (see Results and Discussion).

Subsequent to image normalization, MALDI signal was processed by averaging across smaller regions of interest drawn to correspond with microdissected regions from the corresponding thick slice (cortex, corpus callosum, hippocampus, thalamus, cerebellum gray, and cerebellum white). When comparing MALDI data to the ESI data for the chosen four phospholipids (16:0/16:0 PC, 16:0/18:1 PC, 18:0/18:1 PC, 18:0/22:6 PC), the signal for the molecular species $[M + H]^+$ was added to the corresponding signal for each Na^+ and K^+ adduct ion in each region of interest. The normalized and summed ion abundance for each molecular species was averaged for the four tissue samples to obtain the reported MALDI signal for each PL molecular species.

Normal Phase LC/MS. Electrospray ionization mass spectrometric analysis was carried out using an AB 4000 QTRAP (Applied Biosystems). Normal phase LC was carried out using a flow rate of 200 μL/min on a 2.1 × 150 mm, 5 μm particle size *Acentis* silica column (Supelco; St Louis, MO). Mobile phase A was composed of 30/40 hexane/isopropanol, and mobile phase B was composed of 30/40/10 hexane/isopropanol/10 mM NH_4OAc (aq). Sample extracts (10 μL) were injected, and a gradient was applied over 30 min starting at 40% B, isocratic (5 min), to 60% B (12 min) to 98% B (16 min), isocratic at 98% B (30 min). PC species that were prevalent in both ESI MS analysis and by MALDI mass spectrometric imaging were chosen for analytical comparison.

LC/MS/MS data were acquired in a tandem mass spectrometer in the negative ion mode by selected reaction monitoring (SRM) to ensure molecular specificity in the analysis.[15] The signal for the transition from specific precursor ions (acetate ion adducts) to product (acyl chain) ions were measured. These SRM transitions (16:0/16:0 PC, m/z 792.6 → 255.3; 16:0/18:1 PC, m/z 818.6 → 255.3, 281.3; 18:0/18:1 PC, m/z 846.6 → 283.3, 281.3; 18:0/22:6 PC, m/z 892.6 → 283.3, 327.3) were entered with dwell times of 100 ms for each PC monitored. In separate experiments, these same brain region lipid extracts were analyzed in the positive ion mode by the same normal phase LC/MS and $[M + H]^+$ ion abundances recorded for a PC species.

Processing of Electrospray Data. In cases where two SRM transitions represented a single molecule (precursor ion (acetate adduct) to corresponding acylium ions), the two signals were added together. The calculation of LC/MS/MS abundances was carried out by dividing the SRM signal for each phospholipid target by the signal intensity from the internal standard signal (25 ng; ($[^2H_6]$-16:0/16:0 PC, m/z 798.6 → 258.3). This ratio was then subsequently divided by the weight of the microdissected section and reported as the relative amount of specific phospholipid species/wet weight of tissue. A second method, termed LC/MS/MS relative molar abundance, involved dividing the SRM signal from each target phospholipid by the signal recorded for 16:0/18:1 PC within the dissected sample and results from the 4 separate dissections were averaged and standard errors calculated. The third calculation, termed LC/MS relative molar abundances, was obtained by dividing the abundance of the $[M + H]^+$ for each target phospholipid by the abundance of the $[M + H]^+$ from 16:0/18:1 PC in the dissected sample. This data was in a separate LC/MS analysis of the same tissue extract. The results from the 4 separate dissections were averaged and standard errors calculated.

Statistical Analysis. The relative amounts of specific phospholipid species determined by ESI MS for four tissue samples were averaged for each of the six microdissected regions, and the standard errors were calculated. Similarly, the normalized averaged intensities for phospholipid species recorded in the MALDI MS image were averaged, and standard errors were calculated. Statistical comparison between ESI and MALDI data was carried out with a Pearson product-moment correlation calculation where a value of +1 implies a consistent pattern of change between two independent variables.

RESULTS AND DISCUSSION

Overall Ion Abundances in MALDI IMS. Brain tissue is rich in phospholipids with PC comprising 30 mol % of all phospholipids in rat brain.[16] The averaged mass spectrum acquired (positive ion mode) across the entire surface area of a typical MALDI MS image showed principally phosphocholine molecules as protonated, sodiated, and potassiated adducts (Figure 1A). The major species have previously been identified by collisional activation studies as 16:0/16:0 PC ($[M + H]^+$ m/z 734.6, $[M + Na]^+$ m/z 756.6, $[M + K]^+$ m/z 772.5), 16:0/18:1 PC ($[M + H]^+$ m/z 760.6, $[M + Na]^+$ m/z 782.6, $[M + K]^+$ m/z 798.6), 18:0/18:1 PC ($[M + H]^+$ m/z 788.6, $[M + Na]^+$ m/z 810.6, $[M + K]^+$ m/z 826.6.[5] A small ion at m/z 731.6 has been previously identified as 18:0 sphingomyelin (SM),[5] and the ion at m/z 834.6 has been identified as a phosphocholine molecule consistent with the structure 18:0/22:6 PC.[3] A series of ions at m/z 551.5, 577.5, 605.5, 627.5, and 651.5 were evident in the MALDI spectrum but absent in the ESI spectrum. These ions have been suggested to arise from diacylglyceride molecules ($[M + H - H_2O]^+$)[17,18] but could be in-source fragmentation products of different classes of abundant phospholipids (PE, PI, PS, or PG with acyl chains 16:0/16:0, 16:0/18:1, 18:0/18:1, 18:0/20:4, and 18:0/22:6 respectively) which have been shown to lose the polar headgroup upon collisional activation.[15]

A corresponding electrospray ionization mass spectrum (positive ion) of a Bligh and Dyer extract of an adjacent thick slice of

(14) Hosokawa, N.; Sugiera, Y.; Setou, M. *J. Mass Spectrom. Soc. Jpn.* **2008**, *56*, 77–81.
(15) Pulfer, M.; Murphy, R. C. *Mass Spectrom. Rev.* **2003**, *22*, 332–364.
(16) Sastry, P. S. *Prog. Lipid Res.* **1985**, *24*, 69–176.
(17) Altelaar, A. F.; Klinkert, I.; Jalink, K.; de Lange, R. P.; Adan, R. A.; Heeren, R. M.; Piersma, S. R. *Anal. Chem.* **2006**, *78*, 734–742.
(18) Magnusson, Y. K.; Friberg, P.; Sjövall, P.; Malm, J.; Chen, Y. *Obesity* **2008**, *16*, 2745–2753.

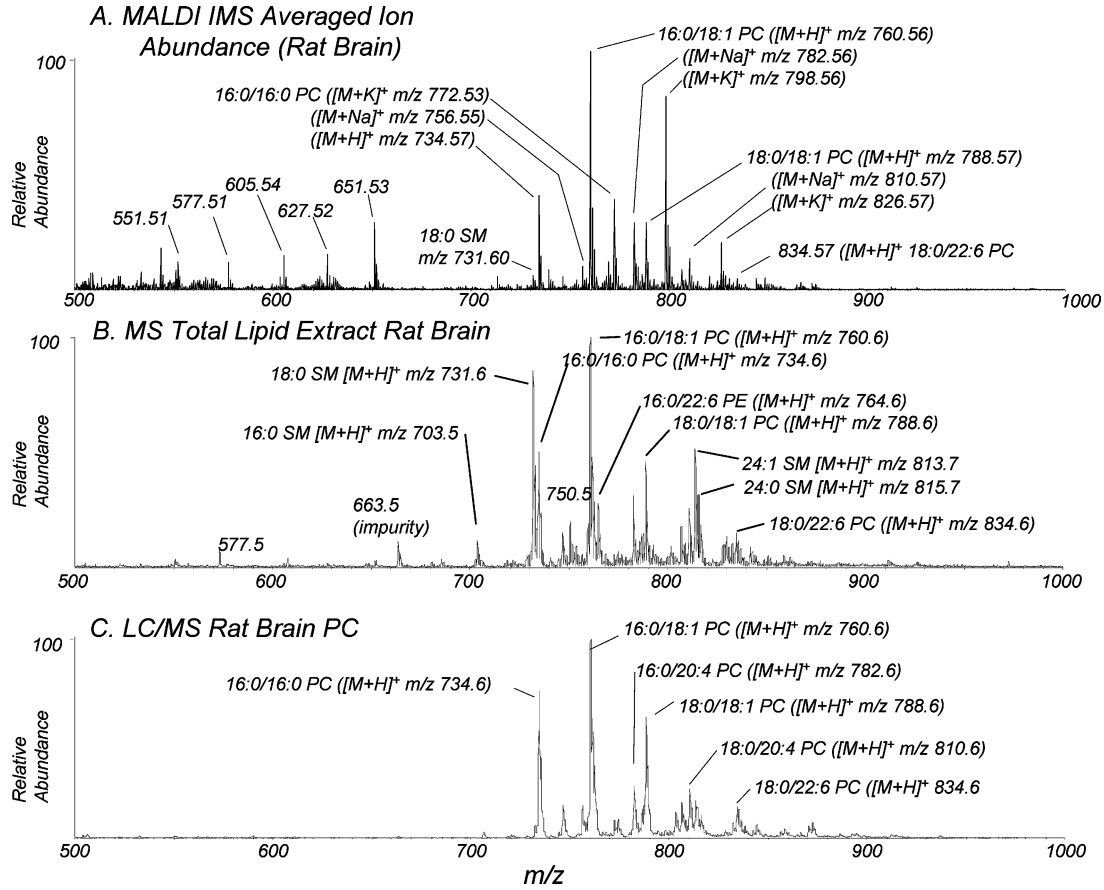

Figure 1. (A) Mass spectrum (positive ion mode) from full MALDI image of rat brain (sagittal section), averaged across entire image. (B) Mass spectrum (positive ion mode) of rat brain extract from electrospray ionization (LC/MS). A sagittal slice of rat brain tissue corresponding to the tissue slice in A was homogenized, and extracted (Bligh/Dyer) and small aliquot (10 μL from 1 mL) was injected into the instrument. (C) Mass spectrum (positive ion mode) of rat brain extract, phosphocholine component from normal phase LC/MS. A sagittal slice of rat brain tissue corresponding to the tissue slice in A was homogenized and extracted (Bligh/Dyer), and small aliquot (10 μL from 1 mL) was injected onto a normal phase HPLC column for phospholipids class separation and mass spectral analysis of components mass range 500−1000 (conditions described in text). The averaged mass spectrum for the phosphocholine region is displayed.

rat brain tissue (Figure 1B) revealed abundant PC molecular species as the MALDI image data with minimal sodium or potassium adducts. Other classes of phospholipids were more apparent such as sphingomyelin species including 16:0 SM $[M + H]^+$ m/z 703.5, 18:0 SM $[M + H]^+$ m/z 731.5, 18:0/24:1 SM at $[M + H]^+$ m/z 813.7, and 18:0/24:0 SM at $[M + H]^+$ m/z 815.7. Phosphoethanolamine (PE) species were detected at m/z 746.5 and 764.6 consistent with 18:0a/18:1 PE and 16:0a/22:6 PE, respectively. These phospholipids yielded an abundant neutral loss of 141 Da following collisional activation (data not shown). The ion at m/z 750.5 fragmented upon collisional activation to form ions at m/z 361 and 390 identifying it as 18:1p/20:4 PE.[19] The LC/MS spectrum of the separated phosphocholine component of the brain extract (Figure 1C) represented the same principle phosphocholine species as the MALDI spectrum without sodium or potassium adducts.

To further examine the hypothesis that image intensity correlated to relative quantity of the analyte measured, MALDI MS image intensities for specific PC molecular species in rat brain sections were compared to semiquantitative measurements of the same PC species in corresponding sections of the tissue. Figure 2A shows the MALDI MS image representing the distribution of the molecule 16:0/16:0 PC $[M + H]^+$ at m/z 734.6 across a sagittal section of rat brain. An adjacent thin slice was H&E stained for structural comparison (Figure 2B). A thick (0.5 mm), adjacent slice was subsequently cut, flash frozen, and used for microdissection of subregions (shown color coded in Figure 2B). Lipids were extracted from each region by standard methods and analysis of phospholipids was carried out by LC/MS tandem methods. Immediately adjacent to the thick cut, the 10 μm slice of tissue was imaged by MALDI IMS (Figure 2C) to establish depth congruency between the microdissected regions from the thick slice and the MALDI MS image. There was consistency in regional intensity patterns of the MALDI MS images comparing the "before" (Figure 2A) and "after" (Figure 2C) slices for m/z 734.6, as well as for all other ions monitored. This implied that the regions where tissue was carved out from the 0.5 mm thick slices (color coded in Figure 2) were contiguous in depth, hence relatable to the two-dimensional displays of the MALDI MS images for each of the four microdissection experiments.

MALDI IMS Comparison to LC/MS for Different Phosphocholine Species Within the Same Region of Rat Brain. The comparison of the intensity of different molecules of the same class within the same tissue region was considered as a simplified

(19) Zemski Berry, K. A.; Murphy, R. C. *J. Am. Soc. Mass Spectrom.* **2004**, *15*, 1499–1508.

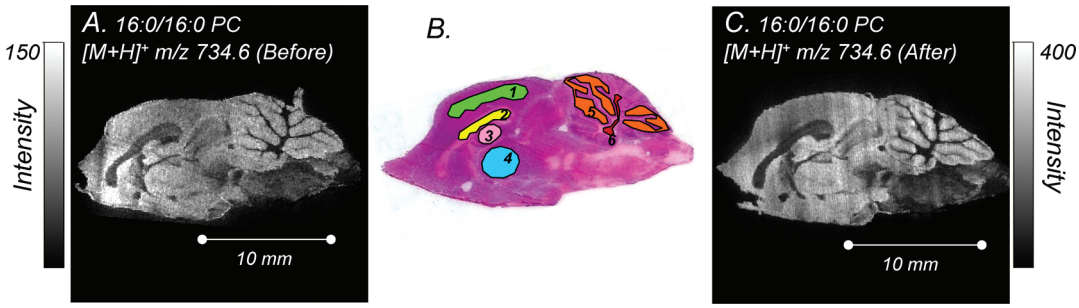

Figure 2. (A) MALDI image of the ion at *m/z* 734.6 (16:0/16:0 PC) from a sagittal section (10 μm thickness) of rat brain sliced before 0.5 mm thick slice (not shown) used for microdissection. MALDI images were acquired at 75 μm pixel size in positive ion mode, DHB matrix applied by sublimation method. The image is shown unsmoothed and unnormalized. (B) An adjacent slice to Figure 2A (10 μm thickness) stained with hematoxylin and eosin (H&E) for visual contrast. Color coded labels 1−6 represent regions from the thick tissue slice (collected between Figure 2A and 2C) that were microdissected, extracted, and analyzed for phospholipid content. Colors and numbers represent the following sections of brain anatomy: region 1 (green) cortex, region 2 (yellow) corpus callosum, region 3 (pink) hippocampus, region 4 (blue) thalamus, region 5 (orange) gray matter of cerebellum, and region 6 (red) white matter of cerebellum. (C) MALDI MS image of the ion at *m/z* 734.6 (16:0/16:0 PC) from a sagittal section (10 μm thickness) of rat brain sliced after 0.5 mm thick slice used for microdissection. MALDI MS images were acquired at 75 μm pixel size in positive ion mode, DHB matrix applied by sublimation method. The image is shown unsmoothed and unnormalized.

Table 1. MALDI IMS Intensities of Phosphatidylcholine ($[M + H]^+$, $[M + Na]^+$, $[M + K]^+$)[a] and Measurement of Each PC Molecular Species in Dissected Rat Brain Cortex by LC/MS/MS)[b]

	PC molecular species			
	16:0/16:0 PC	16:0/18:1 PC	18:0/18:1 PC	18:0/22:6 PC
MALDI IMS $[M+H]^+$	0.16 ± 0.12	0.30 ± 0.20	0.08 ± 0.07	0.023 ± 0.014
MALDI IMS $[M+Na]^+$	0.07 ± 0.013	0.17 ± 0.02	0.07 ± 0.03	0.007 ± 0.001
MALDI IMS $[M+K]^+$	0.30 ± 0.04	0.64 ± 0.21	0.12 ± 0.03	0.022 ± 0.004
MALDI IMS summed signals ($[M + H]^+ + [M + Na]^+ + [M + K]^+$)	0.53 ± 0.09	1.11 ± 0.03	0.27 ± 0.11	0.052 ± 0.016
LC/MS/MS	200 ± 6	190 ± 20	80 ± 20	16 ± 4

[a] MALDI intensity numbers represent net counts for the designated ion, normalized (as discussed in text), averaged across the cortex region of the image then averaged for four separate images. [b] Ion intensities determined by normal phase LC/MS/MS were expressed relative to the signal for internal standard ($[^2H_6]$-16:0/16:0 PC) and divided by microdissected tissue wet weight.

case where MALDI IMS variables of tissue structure, and ion suppression were controlled. A comparison of this type assumed a similar ionization response factor for the ions being compared; a factor that changed substantially with increasing levels of acyl chain unsaturation by LC/MS analysis.[20] Therefore, a quantitative comparison of different ions across the same tissue regions in MALDI MS images could not be done accurately without isotopically embedded labeled internal standards of the same molecular species. The response factors (LC/MS) for 16:0/16:0 PC and 16:0/18:1 PC were similar (data not shown), thus comparisons between these two species was reasonable.

Data for the rat brain cortex region have been collected in Table 1, which displays normalized, numerical MALDI MS ion intensities for four different phosphocholine molecules in each of the adduct forms found in the image ($[M + H]^+$, $[M + Na]^+$, $[M + K]^+$). The raw data intensities were normalized as described in the Methods section because of variability of laser intensity between the four discrete MALDI images. The sum of the adduct forms and the corresponding ESI measured values were also tabulated. The summed MALDI IMS ions for 16:0/18:1 PC were more abundant by a factor of 2 than the summed MALDI IMS ions 16:0/16:0 PC (1.11 relative to 0.53), however, the ESI MS data indicated that the two molecular species were close to equivalent in relative quantity (190:200). This discrepancy could be due to isobaric ions co-ionizing in the MALDI plume at any of *m/z* 760.6, 782.6, and 798.6. Phosphocholine species identified by NP-LC/MS (Figure 1c) as 16:0/20:4 PC ($[M + H]^+$ *m/z* 782.6) could augment the MALDI intensity designated for sodiated 16:0/18:1 PC by up to 20% of the value based on relative peak heights, yet this does not account for the factor of 2 discrepancy. Specific monitoring of the 16:1/18:0 PC isomer by LC/MS resulted in a small signal that was 5% of the signal for 16:0/18:1. Recent ion mobility separation of rat brain extract with high-resolution FT ICR detection resolved the ion at *m/z* 760 in the lipid region to a peptide from an in situ tryptic digest, as well as lipid product.[21] Comparisons of the MALDI IMS intensity of different ions within the same tissue region would be difficult to support without separate knowledge of the ion purity, or specific internal standards.

Comparison of Salt Adducts of 16:0/16:0 PC Across Different Regions of Rat Brain. This study assumed there might be meaningful differentiation in MALDI images related to differences in alkali metal adducts of phospholipids. Preliminary MALDI IMS data of brain tissue showed differences in the distributions of the alkali metal forms of phospholipid species. These differences could indicate subtle differences in tissue structure, tissue pre-

(20) Koivusalo, M.; Haimi, P.; Heikinheimo, L.; Kostiainen, R.; Somerharju, P. *J. Lipid Res.* **2001**, *42*, 663–672.

(21) Stauber, J.; MacAleese, L.; Franck, J.; Claude, E.; Snel, M.; Kaletas, B. K.; Wiel, I. M.; Wisztorski, M.; Fournier, I.; Heeren, R. M. *J. Am. Soc. Mass Spectrom.* **2010**, *21*, 338–347.

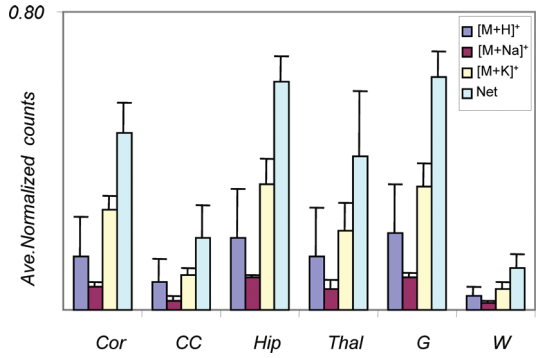

Figure 3. Graphical display of the measured intensity of different (alkali salt adduct) forms of 16:0/16:0 PC ($[M + H]^+$ *m/z* 734.6; $[M + Na]^+$ *m/z* 756.6; $[M + K]^+$ *m/z* 772.6) and their sum averaged over four different MALDI MS images. Data were normalized to the average signal for 16:0/18:1 PC as described in the text. Error bars represent the standard error for four independent measurements.

parations, or disruption of cell membranes upon section cutting. This study retained alkali metal identity of phospholipids rather than pushing the chemical equilibrium of phospholipid ion adducts to single alkali metal species.[4] Matrix was applied by sublimation where the absence of solvent eliminated incidental introduction of sodium or potassium introduced from unpurified matrix, or solvent contact with glass surfaces during spray applications.[3,22] A comparison of the abundances of the different forms ($[M + H]^+$, $[M + Na]^+$, $[M + K]^+$) for 16:0/16:0 PC across brain regions was compiled and shown graphically in Figure 3. There was general agreement in abundance patterns between different regions for the three different forms of the ion, but there was increased variability between regional measurements (larger error bars) for the different salt forms. For example, the hippocampus had nearly twice as much potassium adduct of *m/z* 734 as the M + H form, while the corpus callosum had nearly equal amounts. Given that there were no extraneous additions of salt to the sample from preparations, the inherent distributions of alkali metal adduct forms of phosphocholine molecules were observably different. This might reflect a difference in the location of the lipid within the cell that resulted in greater exposure to potassium ion under experimental and tissue preparation conditions, and invoked a greater incidence of potassium ion adduct formation upon MALDI ablation. The summation of all forms within each MALDI MS image yielded the most reasonable comparisons between different images, implying a normalizing effect when combining all ion forms in the analysis of a phospholipid molecule (see also Table 1).

MALDI IMS and ESI MS Comparison of the Same Phosphocholine Species Across Different Regions of Rat Brain. The comparison of intensity values for a single phosphocholine species within a MALDI MS image across different regions of a rat brain slice controls for variability that might occur related to ionization chemistry. Regions that "look" brighter in MALDI MS images of a specific ion would be expected to have more of the corresponding species when measured independently by LC/MS. This comparison was carried out for four different phosphocholine molecules (16:0/16:0 PC, 16:0/18:1 PC, 18:0/18:1 PC, and 18:0/22:6 PC) across six different tissue regions (cortex, corpus callosum, hippocampus, thalamus, cerebellum gray, cerebellum white) (Table 2).

A graphical display of the data depicted in Table 2 revealed trends when comparing ion abundances across different tissue regions (Figure 4). The MALDI MS image of $[M + H]^+$ *m/z* 734.6 (Figure 4A) had a well resolved contrast between regions of gray matter in the cortex and white matter of the corpus callosum (regions 1 and 2), as well as between gray and white in the cerebellum (regions 5 and 6). For this ion, there was higher ion intensity in the gray matter than in white measured by both ESI and MALDI (Figure 4, A-1, A-2). Regions 3 and 4 were intermediate in value. Dipalmitoyl phosphatidylcholine is a common cell membrane component and the relative differences in the distribution of this molecule depicted in MALDI MS images across different brain regions appeared to be representative of the actual amounts of this molecule present in the tissue.

The ion at *m/z* 760.6 $[M + H]^+$ 16:0/18:1 PC appeared in the MALDI MS image of rat brain (Figure 4B) with greater intensity in regions of gray matter relative to white matter. Specifically, the cortex was brighter than the corpus callosum, and the gray matter folds within the cerebellum were brighter than the corresponding folds of white matter. These trends (Figure 4)B-1 were the same for the measured amounts of this specific species determined by electrospray ionization mass spectrometry (Figure 4)B-2. Interestingly, the corpus callosum was not as distinctly dark for *m/z* 760.6 as for *m/z* 734.6 suggesting that abundance differences between regions were less significant for *m/z* 760.6 than for *m/z* 734.6. The ratio of measured amounts in the cortex relative to corpus callosum for *m/z* 760.6 was 1.8 (MALDI) and the internal standard normalized amounts in the electrospray experiment was 1.6. The ratio of ion abundances in the cortex relative to corpus callosum for *m/z* 734.6 was 2.8 (MALDI) and 2.2 (ESI). The consistency of the ratio when comparing two different molecules over two regions supported the correspondence of the MALDI MS images to the amounts of these phosphocholine molecules.

The ion at *m/z* 834.6 was a phosphocholine molecule identified as the $[M + H]^+$ ion for 18:0/22:6 PC. The distribution shown by MALDI MS (Figure 4C) showed a brighter depiction of this molecule uniquely in the cerebellar gray matter. The relative values measured by LC/MS for 18:0/22:6 PC (Figure 4)C-2 corresponded to the intensities represented in the MALDI IMS image (Figure 4)C-1 with the largest amount of this molecule in the region of the gray matter of the cerebellum. Setou et al.[4] produced high resolution (10 μm pixel size) MALDI IMS images of mouse brain cerebellum that showed an increased intensity for this ion localized to a layer of Purkinje cells within the tissue.[4] The images of other PC molecules that contain a 22:6 acyl chain (16:0/22:6 $[M + H]^+$ *m/z* 806.6, 20:0/22:6 $[M + H]^+$ 862.6) also had increased abundance in the cerebellum gray matter (data not shown). This implied a potential functional significance for esterified docosahexanoate (DHA, 22:6) containing PC related to cerebellar function. An increased abundance of DHA containing phospholipids in retinal rod cells has been associated with an increase in the membrane-embedded, energy-transforming protein, rhodopsin,[23] so perhaps DHA in cerebellum has a specific membrane protein support role as well.

(22) Jaskolla, T. W.; Karas, M.; Roth, U.; Steinert, K.; Menzel, C.; Reihs, K. *J. Am. Soc. Mass Spectrom.* **2009**, *20*, 1104–1114.
(23) Fliesler, S. J.; Anderson, R. E. *Prog. Lipid Res.* **1983**, *22*, 79–131.

Table 2. MALDI IMS Intensities (Sum $[M + H]^+$, $[M + Na]^+$, $[M + K]^+$)[a] and LC/MS/MS Measured Relative Quantities[b] of Phosphocholine Molecules in Rat Brain Regions

	PC molecular species			
	16:0/16:0 PC	16:0/18:1 PC	18:0/18:1 PC	18:0/22:6 PC
MALDI IMS[a] (Cortex)	0.53 ± 0.09	1.11 ± 0.03	0.27 ± 0.11	0.05 ± 0.02
LC/MS/MS[b] (Cortex)	200 ± 6	190 ± 20	80 ± 20	16 ± 4
MALDI IMS (CC)	0.22 ± 0.10	0.65 ± 0.11	0.53 ± 0.14	0.02 ± 0.01
LC/MS/MS (CC)	90 ± 10	100 ± 10	80 ± 20	2 ± 1
MALDI IMS (Hip)	0.68 ± 0.08	1.25 ± 0.07	0.25 ± 0.08	0.04 ± 01
LC/MS/MS (Hip)	200 ± 30	180 ± 40	70 ± 20	7 ± 3
MALDI IMS (Thal)	0.46 ± 0.19	1.12 ± 0.14	0.34 ± 0.05	0.06 ± 0.02
LC/MS/MS (Thal)	150 ± 20	170 ± 20	100 ± 20	10 ± 3
MALDI IMS (G)	0.69 ± 0.08	1.22 ± 0.13	0.24 ± 0.05	0.14 ± 0.03
LC/MS/MS (G)	150 ± 20	150 ± 20	60 ± 10	20 ± 7
MALDI IMS (W)	0.12 ± 0.04	0.55 ± 0.12	0.37 ± 0.11	0.04 ± 0.02
LC/MS/MS (W)	50 ± 20	110 ± 40	60 ± 20	3 ± 1

[a] MALDI intensity numbers represent net counts for the designated ion, normalized (as discussed in text), averaged across the designated region of the image, then averaged (each region) for four separate images. [b] Ion intensities determined by normal phase LC/MS/MS were expressed relative to the signal for internal standard ($[^2H_6]$-16:0/16:0 PC), divided by microdissected tissue wet weight, and averaged over four samples.

The ion at m/z 788 was identified as $[M + H]^+$ for 18:0/18:1 PC.[5] This phosphocholine species consistently had greater intensity in regions of white matter relative to gray by MALDI IMS (Figure 4D). This contrast pattern was unique among other molecules in the phosphocholine class which had signal intensity consistently greater in gray matter than in white. However, the amounts of 18:0/18:1 PC measured by LC/MS did not apparently correlate with the MALDI intensities (Figure 4D-1, D-2) when the signal for this PC species was normalized to tissue wet weight, and instead showed equivalent amounts in the white and gray matter regions. Contributions from isobaric species ($[M + Na]^+$ for 18:0/18:1 PC m/z 810.6 and $[M + H]^+$ for 18:0/20:4 PC) increased the error of the MALDI numerical analysis by the percent this ion added to the sum of signal used for depicting the 18:0/18:1 species. Based on spectral intensities shown in Figure 1, this error was 10−20% but would contribute in the reverse direction as most PC species measured this study were more abundant in gray matter relative to white.

A discrepancy between the MALDI IMS ion abundances in brain regions to that of the phosphatidylcholine concentration (relative abundance/wet weight) assessed in dissected brain regions and measured by LC/MS/MS methods was revealed in a statistical calculation (Pearson's product-moment correlation coefficient) (Table 3). The correspondence values were high between the two measurements for all molecular species except for 18:0/18:1 PC ($r = 0.27$). The low correlation appeared to be localized to regions of white matter and the unique anatomical features of myelin rich white matter. Myelin is known to be highly abundant in white matter and is a tightly packed, dehydrated, and multibilayer membrane[24] with an increased abundance of 18:1 fatty acyl groups in phospholipids.[16] Most importantly white matter PC content is significantly lower when compared to other brain regions.[25] This lower PC concentration in white matter is largely made up by higher sphingolipid content.[26]

This discordance between the MALDI IMS ion abundance and the LC/MS/MS quantitation of PC molecular species in white matter could have been caused by specific factors including the biological presentation of the PC species in myelin, the relatively lower water content in white matter, the use of wet weight in normalization, the ion chemistry of tandem mass spectrometry, tissue surface PC abundance, or integrated PC concentration measured by LC/MS/MS. The effect of expression of electrospray data normalized to wet weight was examined by recalculating the PC abundance as a function of the abundance of 16:0/18:1 PC in the same tissue dissection as others have done.[14,27] The resulting histograms were quite similar for 16:0/16:0 PC and 18:0/22:6 PC but quite different for 18:0/18:1 PC especially in the white matter (Supporting Information Figure 1). Using this calculation, the relative abundance of this latter PC species was significantly higher in the corpus callosum as observed in the MALDI IMS histogram. This approach converted the electrospray data into a measure of molar fraction (relative mole fraction), which was the way the MALDI IMS data was presented. It also removed the bias of white matter having a significantly lower total PC content since every molecular species was measured to that of the signal of a common PC. Statistical analysis revealed that this relative mole fraction assessment brought the comparison between MALDI IMS and LC MS/MS analysis in very close concordance (Figure 4A-3, C-3, and D-3; Table 3). To further examine the effect tandem mass spectrometry and ion chemistry, the electrospray analysis of dissected regions was carried out on an identical aliquot of each brain region by LC/MS analysis which yielded abundances of molecular ion species $[M + H]^+$. The molecular ion abundance for each molecular species was normalized to the 16:0/18:1 PC abundance as above to generate relative mole fraction data (Supporting Information Figure 1). With this approach as well, the IMS and LC/MS data were now in agreement and revealed the unique relative abundance of 18:0/18:1 PC in the corpus callosum and cerebellar white matter (Table 3).

Sphingomyelin and Phosphatidylethanolamine. In contrast to the phosphatidylcholine behavior, there was a noticeable lack of correlation between abundance of SM and PE molecular species in the MALDI image data (Figure 1A) and the electrospray analysis of the total lipid extract (Figure 1B). In part the lack of signals for the PE-related MALDI ions may be related to the instability of the PE $[M + H]^+$ previously mentioned especially because of the relatively high pressure of the MALDI region

(24) Deber, C. M.; Reynolds, S. J. *Clinical Biochem.* **1991**, *24*, 113–134.
(25) Dreissig, I.; Machill, S.; Salzer, R.; Kraft, C. *Spectrochim. Acta A.* **2009**, *71*, 2069–2075.

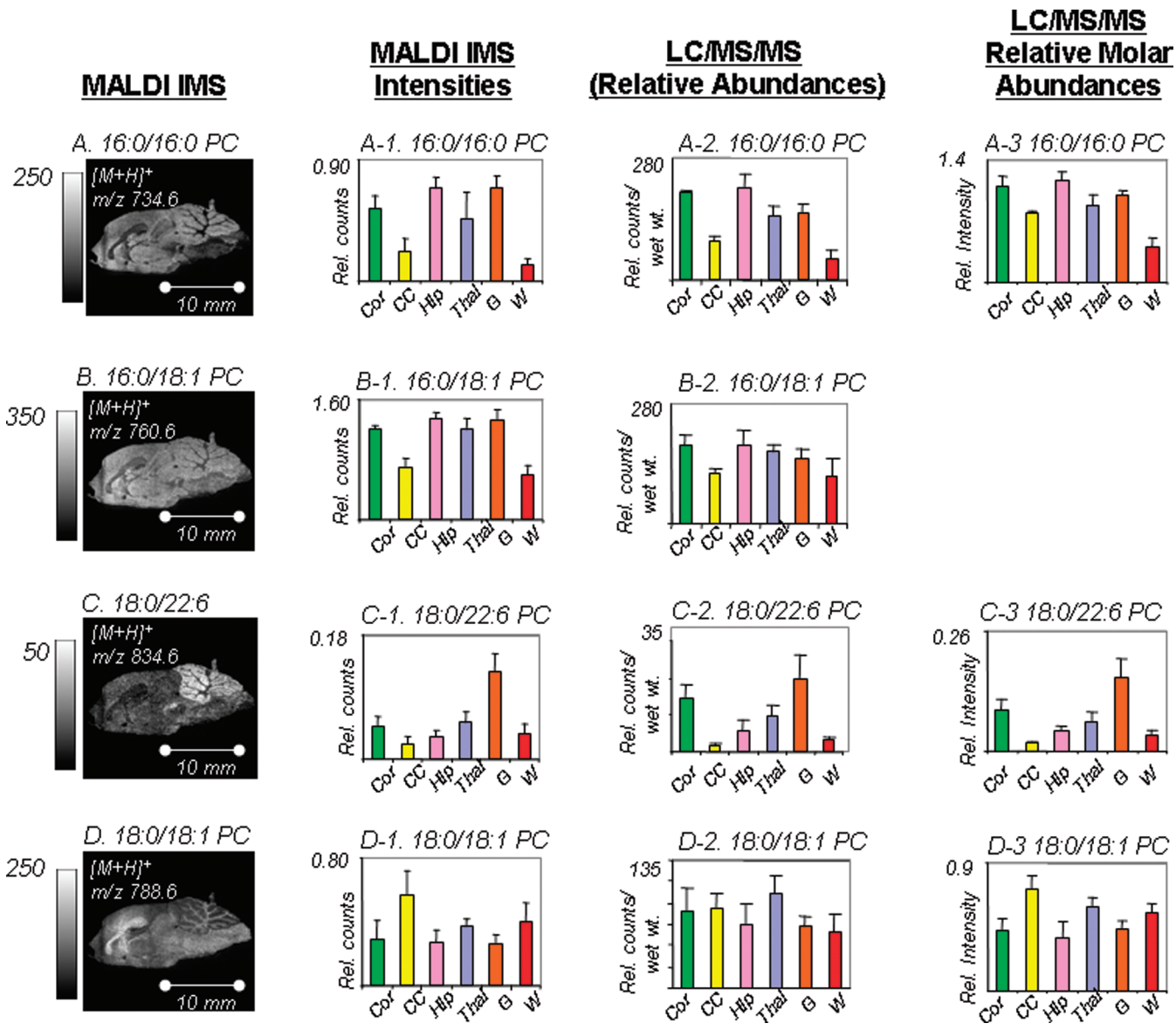

Figure 4. MALDI MS images, MALDI IMS intensities, LC/MS/MS relative abundances and LC/MS/MS relative molar abundances (normalized to 16:0/18:1 PC abundance in tissue) of four different phosphocholine molecules in microdissected regions color coded (green = cerebral cortex, yellow = corpus callosum, red = hippocampus, blue = thalamus, orange = cerebellum gray matter, red = cerebellum white matter). MALDI MS images represent single mass slice of image data set processed to 0.1 amu, displayed without smoothing. MALDI generated numerical ion intensities were processed from four different MALDI MS images, normalized, summed for all forms of the ion ($[M + H]^+$; $[M + Na]^+$; $[M + K]^+$) and averaged to generate standard error measurements shown as error bars on the graph. LC/MS/MS abundances were determined as mass spectrometric signal intensity for analyte ion divided by the signal intensity for the internal standard ($[^2H_6]$-16:0/16:0 PC) as well as divided by wet weight of the microdissected tissue. The numbers displayed represent the averages from separate microdissections of four different thick tissue slices, and error bars show standard error of the set of measurements. (A) MALDI MS image of $[M + H]^+$ *m/z* 734.6 of rat brain sagittal slice. (A-1) MALDI IMS signal intensity for 16:0/16:0 PC positive ions is represented graphically for six different regions of the image. (A-2) LC/MS/MS relative intensity/mg wet weight for 16:0/16:0 PC graphically represented from six microdissected regions of a thick sagittal slice of rat brain. (A-3) LC/MS/MS relative molar abundances for 16:0/16:0 PC normalized to the signal from 16:0/18:1 PC within the same tissue region. (B) MALDI MS image of $[M + H]^+$ *m/z* 760.6 of rat brain sagittal slice. (B-1) MALDI IMS signal intensity for 16:0/18:1 PC positive ions is represented graphically for six different regions of the image. (B-2) LC/MS/MS relative intensity/mg wet weight for 16:0/18:1 PC graphically represented from six microdissected regions of a thick sagittal slice of rat brain. (C) MALDI MS image of $[M + H]^+$ *m/z* 834.6 of rat brain sagittal slice. (C-1) MALDI IMS signal intensity for 18:0/22:6 PC positive ions represented graphically for six different regions of the image. (C-2) LC/MS/MS relative intensity/mg wet weight for 18:0/22:6 PC graphically represented from six microdissected regions of a thick sagittal slice of rat brain. (C-3) LC/MS/MS relative molar abundances for 18:0/22:6 PC normalized to the signal from 16:0/18:1 PC within the same tissue region. (D) MALDI MS image of $[M + H]^+$ *m/z* 788.6 of rat brain sagittal slice. (D-1) MALDI IMS signal intensity for 18:0/18:1 PC positive ions represented graphically for six different regions of the image. (D-2) LC/MS/MS relative intensity/mg wet weight for 18:0/18:1 PC graphically represented from six microdissected regions of a thick sagittal slice of rat brain. (D-3) LC/MS/MS relative molar abundances for 18:0/18:1 PC normalized to the signal from 16:0/18:1 PC within the same tissue region.

in the mass spectrometer employed for these imaging studies. The "diglyceride-like" ions observed could originate from PE molecular species in the brain regions. The lower relative SM signal was noted, but not understood at this time.

Table 3. Correlation of Ion Abundances from MALDI IMS Ions[a] of PC Molecular Species Across Regions of Rat Brain Relative to Ion Abundances of Pc Molecular Species Obtained by LC MS/MS and LC/MS Analysis of Dissected Brain Regions[b]

		Person product moments		
ion	molecular species	LC/MS/MS[c] abundances	LC/MS/MS[d] relative molar abundance	LC/MS[e] relative molar abundance
m/z 734.6	16:0/16:0 PC	0.88	0.90	0.92
m/z 760.6	16:0/18:1 PC	0.88		
m/z 788.6	18:0/18:1 PC	0.27	0.96	0.86
m/z 834.6	18:0/22:6 PC	0.88	0.96	0.76

[a] MALDI ion abundances normalized by abundance of 16:0/18:1 PC averaged over entire brain region. [b] Statistical analysis employed Pearson product moment analysis. [c] Ion intensities of each molecular species obtained by targeted LC/MS/MS (SRM) were normalized to the signal for internal standard ([$^2H_6$]-16:0/16:0 PC) and microdissected tissue wet weight. Averaged over four separate samples. [d] Ion intensities of each molecular species obtained by targeted LC/MS/MS (SRM) were normalized to the signal for 16:0/18:1 PC in the microdissected tissue. Averaged over four separate samples. [e] Ion intensities of each molecular species obtained by LC/MS (full mass scanning) were normalized to the signal for 16:0/18:1 PC in the microdissected tissue. Averaged over four separate samples.

CONCLUSION

MALDI IMS are dramatic and intuitively informative of regional structures of brain tissues. The regional delineation and consistent intensity differences displayed in mass spectrometric images imply a correlation to the true amounts of specific lipid present in the tissue. However, complicating effects related to ionization, salt concentrations, and tissue substructures exist and thereby suggest caution in the interpretation of visual MALDI images as absolute measures. The relative mole fraction of PC species as presented in the MALDI IMS image were in close agreement to the relative mole fractions as determined by LC/MS/MS or LC/MS analysis when the signals were normalized by the abundance of a major PC molecular species. This normalization corrected for significant concentration differences of total PC in regional substructures of the brain and differences due to percent water in the tissue. Although not the topic of this work it is important to point out that abundant signals for PE and SM were determined by the electrospray-based analysis (Figure 1B), but little evidence of those species appeared in MALDI image data of a comparative sample in the positive ion mode (Figure 1A).

For the phosphocholine molecules in the tissue, there are differences in the amounts of alkali metal adducts associated with the molecule within different brain regions as well as from sample to sample. These differences could be due to regional differences in interstitial fluids, or sample preparation that infers more broken cells on a particular tissue slice. Consideration of the distribution of a particular molecular species was most accurate when all ionized forms ($[M + H]^+$, $[M + Na]^+$, $[M + K]^+$) of a molecule are considered together.

There may be other factors pertinent to MALDI IMS image signal intensity in addition to water content of the tissue, tissue organization, and cell structure. Some of these variables will become more apparent as methods of mass spectrometric imaging techniques improve focus to the level of individual cell targets. In general the intensity of any phospholipid species at a specific mass to charge ratio ($I_{m/z}$) appears to be a function of local phospholipid concentration but influenced by phospholipid ion chemistry, local environment in which the lipids are desorbed as well as stability of the MALDI ion species and mass spectrometer instrument factors (e.g., local pressure in the MALDI ion source) and other factors to be determined.

There is much unknown about the functionality of phospholipids in the brain related to details of lipid classes, specificity of acyl chain, acyl chain unsaturation, position on the glycerol backbone, and location within cell membranes. These are potentially meaningful factors of lipid biochemistry for which MALDI IMS will be a useful tool providing a window of focus on the identity and distribution of specific molecules. Further study of specific variables of MALDI imaging will add increased understanding and applicability to this powerful technique.

ACKNOWLEDGMENT

This work was supported in part by a grant from the National Institute of Health Lipid Maps (GM069338). The authors would like to acknowledge the advice from Paul Axelsen (University of Pennsylvania) in brain region dissection, Lara Saba (U01 AA016663 and R24 AA013162) for discussions and statistical assistance, and Erin Genova for assistance in tissue preparations.

SUPPORTING INFORMATION AVAILABLE

Additional material as described in the text. This material is available free of charge via the Internet at http://pubs.acs.org.

(26) Wheeler, D.; Venkata, V.; Bandaru, R.; Calabresi, P. A.; Nath, A.; Haughey, N. J. *Brain* **2008**, *131*, 3092–3102.

(27) Löhmann, C.; Schachmann, E.; Dandekar, T.; Villmann, C.; Becker, C. *J. Neurochem.* **2010**, *114*, 1119–1134.

Received for review April 23, 2010. Accepted August 30, 2010.

AC101079V